Limnol. Oceanogr., 51(1), 2006, 38–46

Distribution of planktonic aerobic anoxygenic photoheterotrophic bacteria in the northwest Atlantic

Michael E. Sieracki
Bigelow Laboratory for Ocean Sciences, P.O. Box 475, 180 McKown Point Road, West Boothbay Harbor, Maine 04575

Ilana C. Gilg
Marine Environmental Biology, University of Southern California, Los Angeles, California 90089-0371

Edward C. Thier and Nicole J. Poulton
Bigelow Laboratory for Ocean Sciences, P.O. Box 475, 180 McKown Point Road, West Boothbay Harbor, Maine 04575

Ralf Goericke
Marine Life Research Group, Scripps Institute of Oceanography, La Jolla, California 92093-0218

Abstract

Aerobic anoxygenic photoheterotrophic (AAP) bacteria can use both dissolved organic matter and light for energy production, but their photosynthesis does not produce oxygen. We measured AAP bacterial cell and bacteriochlorophyll distributions in the northwest Atlantic, from the coast of the Gulf of Maine to the Sargasso Sea, in October 2001 and March 2002. The abundance of AAPs ranged from 7×10^3 to 9.8×10^4 cells mL^{-1} (mean, 2.9×10^4 mL^{-1}) in surface waters, or between 1% and 9% (mean, 2.3%) of total bacteria. Mean abundances in October in the Gulf of Maine (6.6×10^4 mL^{-1}) were about five times higher than those measured in March (1.3×10^4 mL^{-1}), whereas the mean Sargasso Sea values were not different between October and March. AAP cells were larger than other bacteria, so AAP biomass ranged from 2% to 13% of total bacterial biomass. AAP cells were higher in abundance, biomass, and proportion of total bacteria in productive coastal and shelf waters than in the Sargasso Sea. Cell quotas of bacteriochlorophyll were low and quite variable, ranging from 0.02 to 0.17 fg $cell^{-1}$ (mean, 0.08 fg $cell^{-1}$). Our results indicate possible control by temperature and organic and inorganic nutrients on the distribution of planktonic AAPs, but they do not support the idea that they are specifically adapted to oligotrophic conditions.

A unique type of bacterial phototrophic metabolism has recently been shown to be widespread in the ocean (Kolber et al. 2000, 2001; Goericke 2002). These bacteria, termed aerobic anoxygenic photoheterotrophs (AAPs), use bacteriochlorophyll (BChl) *a* but are differentiated from purple and green anoxygenic phototrophs by their requirements for oxygen, synthesis of BChl *a* pigments under dark aerobic conditions, and by their dependence on respiration for energy, with photosynthesis having a stimulatory effect on growth. These cells can use light to fix carbon (Koblízek et al. 2003) and/or to synthesize adenosine triphosphate and nicotinamide adenine dinucleotide phosphate (NADPH), but they do not produce oxygen. They were first isolated from a variety of marine environments by Shiba et al. (1979). Direct cultivation from water samples was rarely successful (0.9% of isolates) relative to isolation from seaweeds and beach sand. Their abundance and significance in the bacterioplankton remained unknown until recently. Their presence in the Sargasso Sea was detected by Britschgi and Giovannoni (1991), who used gene cloning and sequencing and who hypothesized that their metabolism could be important in the ocean. Their widespread distribution in the aerobic ocean is remarkable, since bacteria with this photosystem was previously known to dominate only in specialized environments associated with low oxygen but adequate sunlight, such as stratified lakes and microbial mats (Fenchel et al. 1998). The genetic operon coding for the BChl *a* photosynthetic apparatus has been shown to exist in a diverse range of marine *Proteobacteria* from the α and γ classes (Béjá et al. 2002). They can use both light and organic matter for energy production. The diversity and ecology of this group has recently been reviewed by Rathgeber et al. (2004).

With two potential energy and carbon acquisition pathways, it was suggested that they would be most abundant where overall community productivity and organic matter are low, such as in the oligotrophic open ocean (Kolber et al. 2000; Karl 2002). There they could outcompete other bacteria by using light energy in addition to respiration and could outcompete phytoplankton for inorganic nutrients because of their small cell sizes. This idea is supported by observations from eastern Pacific waters off the coast of California, where BChl *a* to chlorophyll *a* (Chl *a*) ratios were

Acknowledgments

We thank Capt. Dick Hogus and the crew of the R/V *Cape Hatteras*. Brian Thompson, Rich Entel, Renée Lagasse, and Helga Gomes prepared samples and measured Chl *a* on the cruises. Zbignew Kolber provided microscope advice. Robert Guillard provided a critical review of the manuscript. Funding was provided by the U.S. National Science Foundation Biological Oceanography and Small Grants for Exploratory Research programs (OCE-9986331, OCE-0225975).

highest where Chl *a* was low (Goericke 2002). Similarly, measurements using infrared fast repetition rate fluorometry (Kolber et al. 2000) showed higher BChl *a* signals in the more oligotrophic waters of the eastern Pacific off the coast of Mexico. Observations of the vertical distribution of cells in the northeast Pacific revealed higher abundances in the surface mixed layer of the water column (Kolber et al. 2001).

We report here AAP cell distributions and BChl *a* concentration across a strong trophic gradient, as defined by Chl *a* concentration, from the productive, coastal Gulf of Maine waters to the oligotrophic northern Sargasso Sea. We used infrared fluorescence microscopy combined with digital image analysis to count and size total bacteria and the AAP cells. We found that AAP abundance, biomass, and proportion of total bacteria were higher in the more productive, coastal waters than in the oligotrophic Sargasso Sea, indicating that they are not specifically adapted to oligotrophic conditions.

Materials and methods

We examined samples from two cruises in the northwest Atlantic, on transects from coastal waters of the Gulf of Maine to the vicinity of Bermuda in the northwest Sargasso Sea. Cruise CH-0301 took place from 13 to 25 October 2001 and cruise CH-0402 took place from 7 to 28 March 2002.

Sampling—At each station a drifter was deployed with a drogue at 15 m to track the water at that depth. Fifteen meters was chosen to represent the surface mixing layer across the different water types. At all stations, 15 m was well within the mixing layer based on the vertical density profiles measured by a conductivity, temperature, depth (CTD) probe. As weather permitted, two samples were taken at each drifter station about 24 h apart. Samples were collected with Niskin bottles on a rosette with a CTD instrument. On the March cruise, subsamples for BChl *a* pigment analysis were filtered onto 25-mm GF/F filters. Two liters of water were filtered for the coastal and shelf samples and 4 liters for the Sargasso Sea samples. Filters for pigments were placed in cryovials, immediately placed in liquid N_2, and stored until analysis. Subsamples for microscopy were fixed with glutaraldehyde (0.3%, final concentration). Slides were prepared 1 to 24 h after fixation using standard methods for epifluorescence microscopy (Porter and Feig 1980). Three to twenty–milliliter subsamples were stained with 4′,6-diamidino-2-phenylindole (DAPI) (5 μg mL^{-1}, final concentration) and filtered onto black polycarbonate filters (pore size, 0.2 μm). The filters were mounted on slides, and a small drop of immersion oil and a cover slip were added. The slides were frozen until analysis after the cruise. Glutaraldehyde, DAPI, and rinse water were filtered (pore size, 0.2 μm) daily, and blank slides were checked for contamination.

Phototrophic pico- and nanoplankton were enumerated within 2 h of collection using a B-D FACScan benchtop flow cytometer on live samples. Total Chl *a* was determined fluorometrically by filtering samples onto GF/F filters, extracting in 90% acetone for 24–48 h in the freezer, and reading fluorescence on a calibrated Turner Design fluorometer (Parsons et al. 1984).

BChl *a* was measured after acetone extraction with reverse-phase, high-pressure liquid chromatography and was detected by its characteristic absorption peak at 770 nm (Goericke 2002).

Microscopy—A Zeiss Axioskop microscope was used to image bacteria. It was equipped with a Photometrics CH-250 cooled, slow-scan, infrared (IR)-sensitive charge coupled device (CCD) camera with 1,317 × 1,034 pixels (Roper Scientific), interfaced to a Macintosh G3 computer (Apple Computer). The microscope used a mercury lamp for excitation. Schwalbach and Fuhrman (2005) found that a xenon lamp more efficiently excited the IR fluorescence of BChl *a.* Such a light source was not available to us, and our long exposure times (below) probably compensated for the weaker excitation by the mercury lamp. Three epifluorescence filter sets were used: (1) RG 850-nm emitter, FT 650-nm dichroic, and 375–550-nm exciter to detect the infrared emission of BChl *a*; (2) LP 520-nm emitter, FT 510-nm dichroic, and 450–490-nm (blue) exciter to detect Chl *a* and divinyl Chl *a*; and (3) LP 450-nm emitter, FT 425-nm dichroic, and 390–420-nm (violet) exciter to detect DAPI. Images were acquired using a Zeiss 63X Plan-Neofluar objective (1.25 NA) yielding a resolution of 0.11 μm per pixel. IPLab Spectrum image analysis software (Scanalytics, Inc.) was used for camera control and image analysis. Each day, camera bias, flat-field, and fluorescence calibration images were acquired for each optical filter set to account for any changes in camera response, illumination, etc. Microscope fields were selected at random, except for a few instances in which large phytoplankton cells or detrital particles dominated the field of view. In these cases, these slides were scanned by eye, and fields with fewer large particles were chosen. Initial focus was performed using IR optics, except when the IR fluorescing particles were too few to be captured in a focus window, in which case focus was performed using the DAPI optics (violet excitation). For each field of view, the IR image was captured first, requiring a 15–20-s exposure, followed by the Chl *a* (blue excitation, 2-s exposure) and the DAPI (violet excitation, 1-s exposure) images.

Images were flat-field and bias corrected (Viles and Sieracki 1992) and then normalized for display, and the Chl *a* and IR image pairs were merged into a single two-color image (Fig. 1). AAP-positive cells were functionally defined as those with IR fluorescence values of at least three times that of the corresponding values in the Chl *a* image, at least three times the average background value, and those that possessed a corresponding signal in the ultraviolet-DAPI image (Table 1). Chl *a* was also detected in the IR images. This could have been due to a weak emission tail of Chl *a* in the infrared, or a less-than-perfect optical cut-off filter, combined with the high camera sensitivity. So small Chl *a*–containing cells (e.g., pico-eukaryotes and *Prochlorococcus*) could easily be confounded with AAPs if only the IR image was observed. Cells containing Chl *a* were identified in the Chl *a* images and were not counted. AAP cells were counted visually from the computer display, and the cell morphologies were noted.

Total bacteria counts were done by flow cytometry using PicoGreen (Molecular Probes, Inc.) for the October cruise

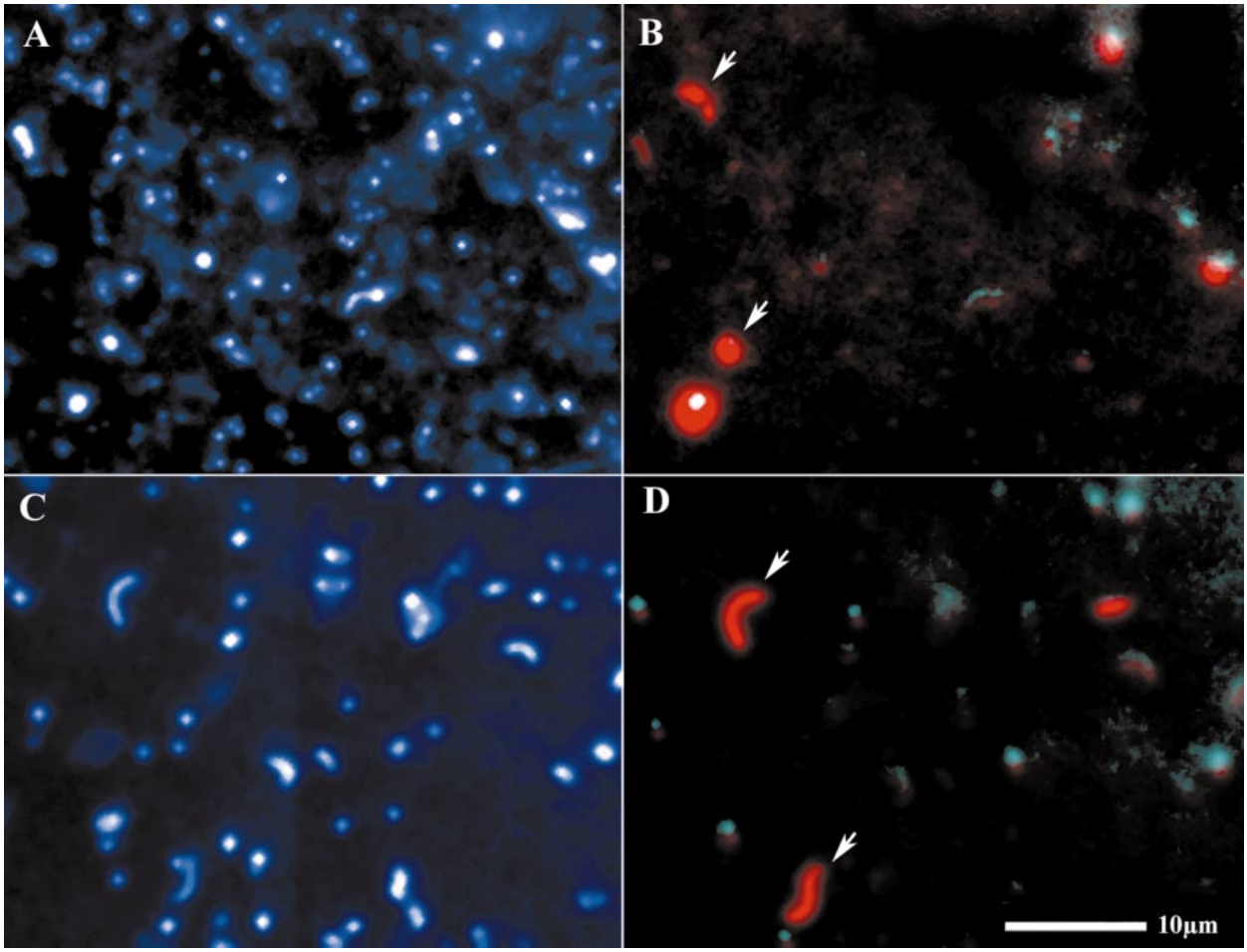

Fig. 1. Selected digital images of AAPs from (A and B) Georges Bank and (C and D) Sargasso Sea. Panels A and C show the total bacterial population stained with DAPI. Panels B and D are dual-image overlays showing AAP cells under infrared fluorescence as red (arrows) and chlorophyll *a* (Chl *a*) or divinyl Chl *a* fluorescence under blue excitation as cyan. The large bright cell in the upper left of panels A and B is a *Synechococcus* cell. The dim cyan cells in D are *Prochlorococcus.*

(CH-1301) and by image analysis from DAPI images (Viles and Sieracki 1992) for March (CH-0402), because of PicoGreen staining problems. Cell counts by microscopy and flow cytometry have been shown to be comparable (Sieracki et al. 1999; Ducklow et al. 2001). Cell biovolumes were measured by image analysis using the DAPI images and previously described algorithms (Sieracki et al. 1989; Viles and Sieracki 1992). AAP cell sizes were measured in their corresponding DAPI images to compare with total bacteria. We use the term total bacteria for the DAPI count, acknowledging that it includes *Prochlorococcus* (Sieracki et al. 1995) and Archaea (Karner et al. 2001), but not *Synechococcus* (which are distinctive in size and phycoerythrin fluorescence). Biomass was calculated from biovolume using a bacterial carbon density factor of 220 fg C μm^{-3} (Fry 1988). Biomass values calculated using this constant were near the midpoint of those calculated using two recently determined power functions (Posch et al. 2001; Gundersen et al. 2002).

Table 1. Scheme used to detect and distinguish AAP bacteria in epifluorescence microscope images from other small cells.*

Filter set (Ex, DT, Em)	DAPI (390–420, 425, 450)	Chl *a* or divinyl Chl *a* (450–490, 510, 520)	Infrared BChl *a* (375–550, 650, 850)
Heterotrophic bacteria	++	—	—
Prochlorococcus	+	+	+
Synechococcus	+	++	+
Picoeukaryotes	++	++	+
AAP bacteria	++	—	+ or ++

* Ex, excitation bandpass filter; DT, dichroic mirror cutoff; Em, emission long pass filter; —, no signal; +, signal seen; ++, strong signal. Values are wavelengths in nm.

Results

AAP cell concentrations varied by a factor of 14, ranging from about 7×10^3 to over 9.8×10^4 cells mL^{-1} (Table 2), while total bacteria varied by a factor of 8, from 0.5×10^6 to 3.9×10^6 cells mL^{-1}. The highest concentrations of AAPs ($>7 \times 10^4$ mL^{-1}) were found in the stratified, productive

Table 2. Station locations, environmental variables, and AAP abundances and morphology. All samples were taken from depths between 11 and 15 m. Between 100 and 400 AAP cells were counted per sample (mean, $n=265$). The majority of AAPs were short rods.*

Cruise, dates, and station	Latitude °N	Longitude °W	T °C	Chl *a* (μg L^{-1})	Total bacteria (10^6 mL^{-1})	AAPs (10^3 mL^{-1})	Vibrio and spirilla AAPs (%)
CH-1301, 13–25 Oct 2001							
EMCC	44°5.1′	68°0.8′	10.37	1.35	1.03	30.0	—
EMCC	44°2.7′	68°3.3′	10.57	1.86	1.27	34.9	—
Jordan Basin	43°30.7′	67°36.4′	11.67	2.29	3.90	98.4	1
Jordan Basin	43°29.6′	67°34.8′	11.59	1.37	2.18	53.3	—
Wilk. Basin	42°38.1′	69°47.8′	12.94	1.46	2.51	63.0	—
Wilk. Basin	42°36.0′	69°47.6′	12.77	1.84	2.71	81.7	—
Georges Bank	40°55.4′	67°35.4′	14.66	2.83	1.29	75.7	—
Georges Bank	40°55.1′	67°39.2′	14.70	2.16	1.00	93.6	1
Gulf Stream	37°55.4′	68°44.1′	25.15	0.17	0.95	21.6	11
Gulf Stream	37°39.9′	68°10.8′	25.00	0.28	0.95	27.5	14
Sargasso 1	35°41.7′	68°17.9′	24.20	0.12	1.21	10.1	36
Sargasso 1	35°29.2′	68°17.7′	24.24	0.09	0.70	10.9	40
Sargasso 2	36°51.4′	69°53.6′	23.97	0.11	0.49	12.6	36
Sargasso 2	36°54.8′	69°46.4′	23.92	0.12	0.77	8.2	32
CH-0402, 7–28 Mar 2002							
EMCC	44°4.9′	68°1.5′	4.10	ND	1.05	13.2	1
EMCC	44°7.4′	68°2.9′	4.02	2.43	0.97	10.9	—
Jordan Basin	43°29.2′	67°37.3′	4.21	0.72	0.91	7.6	—
Wilk. Basin	42°38.1′	69°48.5′	5.54	0.97	0.98	10.4	1
Wilk. Basin	42°38.1′	69°48.7′	5.40	0.96	1.26	13.1	1
Georges Bank	40°53.7′	67°36.8′	5.92	1.65	1.05	21.0	3
Sargasso 1	35°44.4′	68°21.1′	21.05	0.45	0.69	10.6	8
Sargasso 1	35°45.0′	68°31.3′	21.01	0.43	0.82	13.0	10
Sargasso 3	33°29.8′	65°50.0′	19.26	0.28	0.60	14.9	6
Sargasso 3	33°21.4′	65°53.7′	19.36	0.16	0.53	8.0	7
Sarg. BATS	31°48.0′	63°60.0′	20.07	0.11	0.54	7.1	17
Sarg. BATS	31°50.8′	63°59.0′	20.02	0.14	0.40	7.9	11

* EMCC, Eastern Maine Coastal Current; Wilk., Wilkinson; Sarg. BATS, near Bermuda Atlantic Time-Series Study Station; —, type not detected or less than 1% of total; ND, no data.

Gulf of Maine waters of the Jordan and Wilkinson Basins and on Georges Bank in October. The lowest concentrations (<8,000 mL^{-1}) were found in the Sargasso Sea and in the colder, low–Chl *a* water of the Jordan Basin in March. Mean abundances of the eight samples from the Gulf of Maine in October were 6.6×10^4 mL^{-1}, about five times higher than the mean there in March (1.3×10^4 mL^{-1}, $n = 6$). In contrast, the mean Sargasso Sea abundances were not significantly different between October and March, at 10.4×10^4 mL^{-1} ($n = 4$) and 10.2×10^4 mL^{-1} ($n = 6$), respectively. The contribution of AAPs to total bacterial numbers ranged from 0.8% to 3%, except for the two Georges Bank samples in October, where these numbers constituted 6% and 9% of the total bacterial population. The overall mean ratio of AAPs to total bacteria for these surface samples over the two cruises was 2.3%.

In March, high Chl *a* levels and numbers of AAPs at the Sargasso 1 station (Table 2) coincided with a diatom bloom observed there following a storm. The high winds of the storm presumably mixed nutrients into the surface layer, resulting in a short-term bloom that yielded higher Chl *a* levels and AAP numbers. Such events occur at the nearby Bermuda Atlantic Time-Series Study (BATS) site about every 5 yr (Steinberg et al. 2001). The ship followed the drifter into a different water mass over the 24-h period at the Sargasso 3 station, which accounts for the difference in AAP abundance between the two samples at that station (Table 2). The first CTD rosette cast there yielded high Chl *a* levels and AAP numbers and the highest percentage AAPs of total bacteria (2.5%) seen on the March cruise. Warmer, saltier water with lower Chl *a* content and lower AAP abundances were found in the samples from the second CTD rosette cast at the Sargasso 3 station.

The morphologies of AAPs in coastal and shelf waters were predominantly short rods (Table 2), while in oligotrophic waters they showed a diversity of shapes, including vibrio and spirilla (Fig. 2), especially in the warmer October samples. However, in the Sargasso Sea samples, many vibrio and spirilla did not show BChl *a* fluorescence, so these morphologies are not distinctive for AAPs. AAPs from the October cruise accounted for only about 15–30% of the bacteria with these distinctive morphologies.

Cell sizes (biovolumes) of AAPs and total bacteria were measured from Sargasso Sea, Georges Bank, and eastern Maine coastal current samples. AAP cells were distinctly larger than the total bacterial population at all stations (Table 3; Fig. 3). Because of their consistently larger cell size, the AAPs constituted a larger proportion of bacterial biomass

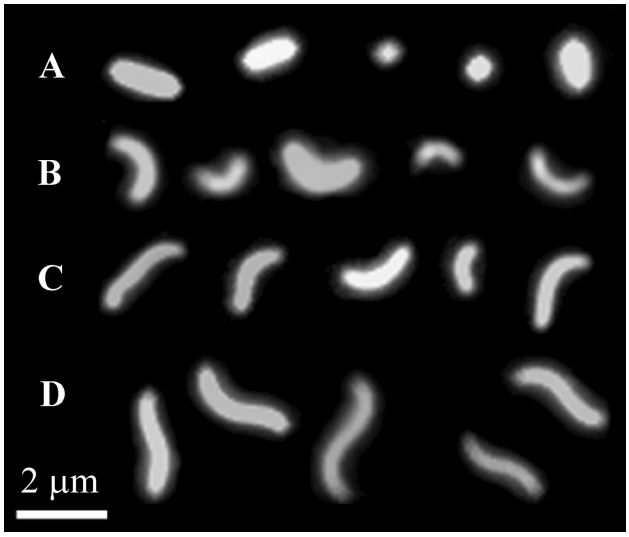

Fig. 2. Commonly observed morphological types of AAP cells from infrared fluorescence images: (A) short rods; (B and C) vibrio; and (D) spirilla.

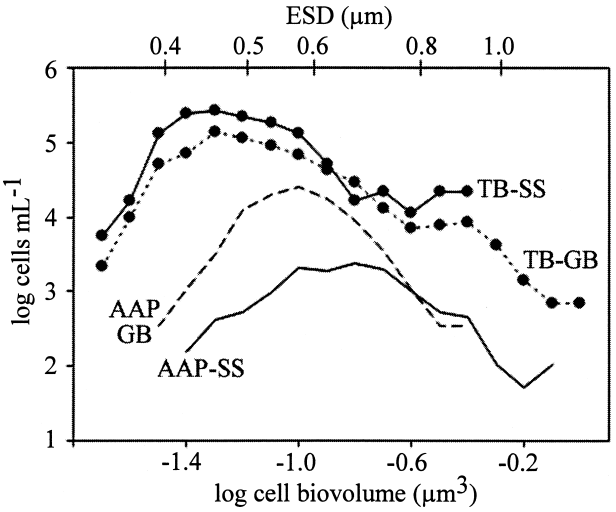

Fig. 3. Comparison of size spectra of total bacteria (DAPI counts) and AAP bacteria from the October cruise (CH-1301). ESD, equivalent spherical diameter calculated from biovolume; TB, total bacteria; SS, Sargasso Sea 2; GB, Georges Bank. Bin width is 0.1 log units. Counts are normalized to cells mL^{-1} for direct comparison.

than their abundance alone would indicate. For example, on Georges Bank in October, they comprised almost 13% of the bacterial biomass, whereas they were 6% to 9% of total cell numbers (Table 2).

The vertical structure of the Sargasso Sea water column in October showed a Chl *a* maximum in the thermocline at about 75 m (Fig. 4). AAP cell abundances had a maximum of 1.1×10^4 to 1.3×10^4 cells mL^{-1} between 15 and 60 m. Surface abundances were lower, at 8×10^3 cells mL^{-1}, and abundances declined quickly below the thermocline. This pattern generally paralleled the vertical distribution of total bacteria, except that AAP numbers were lower at the surface, and they declined more rapidly with depth below the Chl *a*

Table 3. Mean cell biovolumes and biomass for total bacteria and AAPs from selected surface samples. Biovolumes were determined from the two-dimensional digital images by a simple computational rotation around the longest axes. Biomass is calculated using a density factor of 220 fg C μm^{-3}.*

Cruise Station	Mean cell biovolume (μm^3)		Biomass (μg C L^{-1})		
	TBac	AAP	TBac	AAP	%AAP
CH-0301 Oct 2001					
EMCC	0.05	0.13	14.35	1.00	7.0
Georges Bank	0.07	0.09	14.93	1.93	12.9
Sargasso 1	0.08	0.17	12.12	0.41	3.4
Sargasso 2	0.08	0.15	8.35	0.41	5.0
CH-0402 Mar 2002					
EMCC	0.10	0.16	20.79	0.37	1.8
Georges Bank	0.08	0.11	19.26	0.48	2.5
Sarg. -BATS	0.08	0.15	9.67	0.23	2.4
Sarg. -BATS	0.08	0.12	6.53	0.21	3.3

* %AAP, percent of total bacterial biomass; Tbac, total DAPI count; station abbreviations as in Table 2.

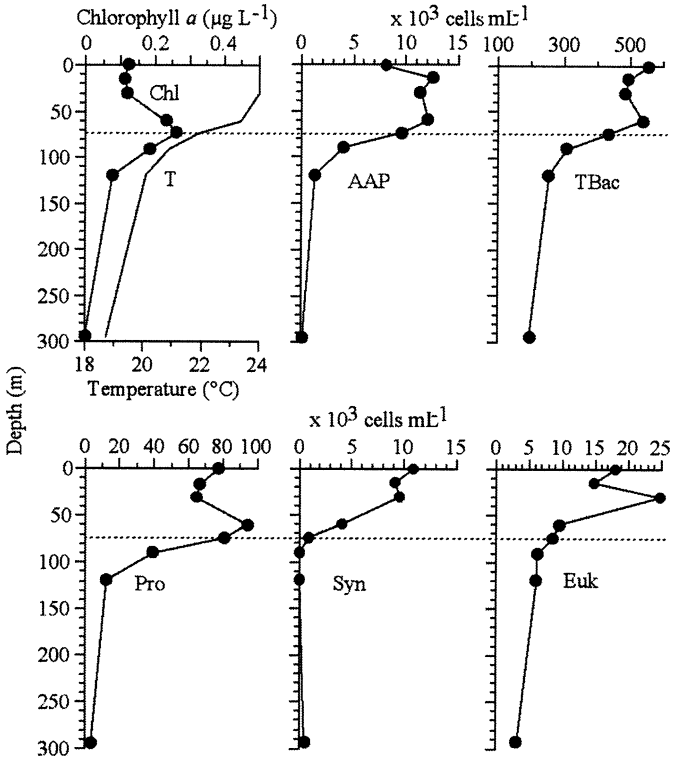

Fig. 4. Vertical profiles of AAPs along with chlorophyll (Chl *a*), temperature (T), and the major groups of microorganisms at the October cruise (CH-1301) Sargasso Sea 2 station. Tbac, total bacteria; Pro, *Prochlorococcus*; Syn, *Synechococcus*; Euk, small (<20 μm) phototrophic eukaryotes. The dashed line indicates the Chl *a* maximum at 74 m.

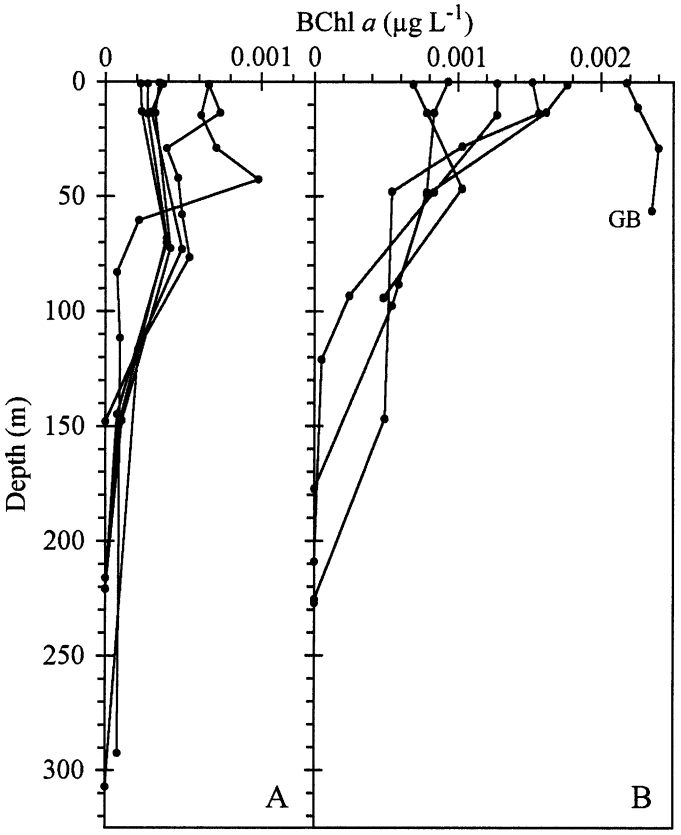

Fig. 5. Vertical profiles of BChl *a* concentrations for the March cruise (CH-0401): (A) Sargasso Sea and (B) Gulf of Maine; GB identifies the Georges Bank profile.

maximum. At 119 m, AAPs were about 10% of their maximum, while the total bacterial population was about 50%, and at 294 m, AAPs were 1% and total bacteria were 35% of their respective surface maxima. The phototrophic components of the microbial community also showed maxima in the surface layer, as expected (Fig. 4). The depths of maximum cell abundances of *Prochlorococcus* and other eukaryotes were at 60 and 30 m, respectively, while the *Synechococcus* abundance maximum was at the surface.

Vertical profiles of BChl *a* concentrations from the March cruise showed higher values in the surface and low values, often near the detection limit, below 100 m (Fig. 5). Concentrations of BChl *a* in the Sargasso Sea were mostly below 1 ng L^{-1} (Fig. 5A), whereas many surface layer values from the Gulf of Maine were above 1 ng L^{-1} (Fig. 5B). At all depths sampled, the BChl *a* concentrations at Georges Bank were above 2 ng L^{-1}, the highest observed. BChl *a* was highly correlated with Chl *a* on this cruise (r^2 = 0.98, n = 65).

For the March cruise samples in which we had both BChl *a* concentrations and AAP cell abundances, the BChl *a* concentrations showed more variation than did the AAP cell abundances (Table 4). BChl *a* levels ranged from 0.23 ng L^{-1} at the Sargasso BATS station to 2.25 ng L^{-1} on Georges Bank. The calculated cell quotas of BChl *a* averaged 0.08 fg BChl *a* cell^{-1} and ranged from 0.02 to 0.17 fg BChl *a* cell^{-1}. Although the highest cell quota we observed was in

Table 4. Concentrations of AAP cells and BChl *a* and resulting cellular quotas for selected surface samples from the March cruise (CH-0402). Station abbreviations as in Table 2.

Station	AAP cells (10^3 mL^{-1})	BChl *a* (ng L^{-1})	Cellular quota (fg BChl *a* cell^{-1})
EMCC	13.2	0.83	0.06
EMCC	10.9	0.78	0.07
Jordan Basin	7.6	1.27	0.17
Wilk. Basin	10.4	1.62	0.16
Wilk. Basin	13.1	1.57	0.12
Georges Bank	21.0	2.25	0.11
Sargasso 1	10.6	0.61	0.06
Sargasso 1	13.0	0.74	0.06
Sargasso 3	14.9	0.32	0.02
Sargasso 3	8.0	0.29	0.04
Sarg. BATS	7.1	0.27	0.04
Sarg. BATS	7.9	0.23	0.03
Mean	11.5	0.90	0.08
St. Dev.	3.9	0.65	0.05
C.V. (%)	34	72	64

Jordan Basin and the lowest was the Sargasso 3 station, there was no consistent relationship between cell pigment content and trophic status of the stations. Normalizing the pigment content to cell volume also did not show a particular relationship across stations. The average was 0.59 fg BChl *a* μm^{-3}, and values ranged from 0.16 fg BChl *a* μm^{-3} in the Sargasso 1 sample to 1.26 fg BChl *a* μm^{-3} at Jordan Basin.

Across the trophic gradient in October, the abundance of AAPs appears to be correlated with Chl *a* concentration (r^2 = 0.78; Fig. 6). Samples from the two eastern Maine coastal current stations from October, which were the coldest stations sampled on that cruise, fell below the regression line,

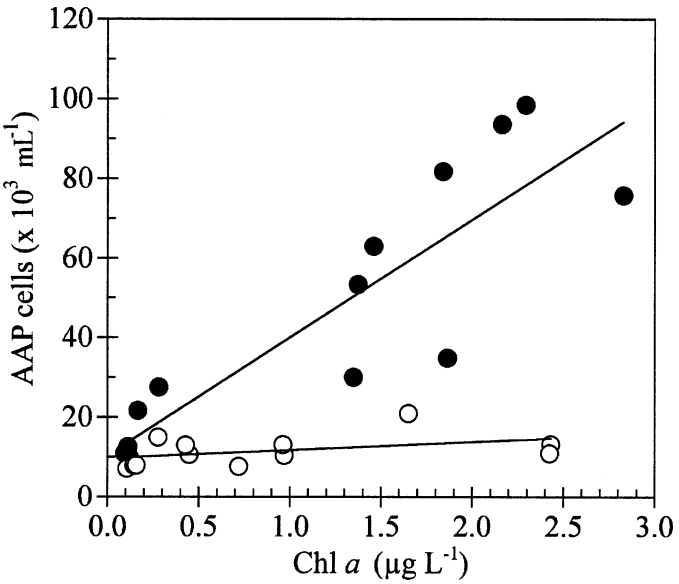

Fig. 6. Relationship between AAP cell numbers and chlorophyll *a* (Chl *a*). Closed circles are October and open circles are March cruise samples. Lines show linear regressions calculated for each cruise. October r^2 = 0.78 and March r^2 = 0.17.

having fewer cells than other stations in the mid-range of Chl *a* levels. In the winter cruise (March), AAP populations did not increase with Chl *a*, although the highest abundance of AAPs was still seen at Georges Bank. High Chl *a* levels (i.e., >1 μg L^{-1}) were found in the Gulf of Maine and Georges Bank stations in March, where temperatures there were all below 6°C (Table 2), indicating that low temperature may limit AAP cell abundances. In contrast, the temperatures in the Gulf of Maine in October, where the highest AAP abundances were seen, were all above 10°C. The coastal stations showed the greatest differences in AAP abundances between the two seasons. The mean AAP cell abundances for the Sargasso stations were not significantly different (1.048×10^4 mL^{-1} [SE 1,070] in October vs. 1.027×10^4 mL^{-1} [SE 1,414] in March).

Discussion

There are several major differences between this study and previous ones: (1) we studied a stronger trophic gradient; (2) our observations are for the North Atlantic; (3) we saw differences in temperate waters with time of year; (4) we focused on directly measured cell abundances and sizes across the trophic gradient; (5) we measured AAP cell sizes; and (6) we compared AAPs to total bacterial abundance and biomass. Measurements of in vivo IR fast repetition rate fluorometry (Kolber et al. 2000) as a proxy for cell distributions can be confounded by the variations in both cell photophysiology and pigment per cell. Our calculated pigment to cell ratios indicate high variability. Our observations, especially those for October, differ from previous observations in the eastern North Pacific, where the relative abundance of AAPs is inversely correlated with Chl *a* (Kolber et al. 2000, 2001). The hypothesis that their ability to use both light and organic matter simultaneously for energy would give them a competitive advantage over other bacteria in low-productivity waters (Karl 2002) may need revision.

The abundances we observed, ranging from 0.7×10^4 to 9.8×10^4 mL^{-1}, compare favorably to the range seen by Kolber et al. (2001) in the northeast Pacific (1×10^4 to 9×10^4 mL^{-1}). Similarly, Schwalbach and Fuhrman (2005) found cell abundances from near zero to 4×10^4 cells mL^{-1} in a vertical profile off the coast of southern California. The infrared fluorescence microscopy method used here and in the Kolber and Schwalbach studies could include cells other than AAPs that contain BChl *a*, in particular purple bacteria. These bacteria, however, are inhibited by oxygen and usually grow in anoxic environments. Given the high grazing rates by microflagellates in the ocean, it is not likely that a residual population of such cells would persist.

Over a 2.5-yr time sequence in the San Pedro Channel, Schwalbach and Fuhrman (2005) found that AAPs varied from 0.05% to 6.3% (mean, 1.2%) of the total bacteria population; however, most values were less than 1%. Using a different method, quantitative polymerase chain reaction measurements of gene copies, they examined a set of 18 samples from a wide range of marine habitats around the world. They found percentages of AAPs to total bacteria of less than 1% for 12 of the 18 samples tested, although two estuarine/coastal samples were at 11% and 19%. Generally higher ratios were found by Kolber et al. (2001), ranging from 1.2% to 14.9%, with a mean of 6.0%. So our measurements fall between these two other studies, with a mean of 2.3% (range, 0.8–9%).

The morphological diversity of AAPs we observed in the oligotrophic samples is interesting, since high genetic diversity of marine bacteria containing the genes for AAP photophysiology has been observed (Béjá et al. 2002), and genetic and morphological diversity of bacteria is not necessarily correlated. Diverse morphologies of these bacteria have been observed in isolates from lakes, and a pleomorphic form that can grow in a Y-shape was isolated from the vicinity of a deep-sea hydrothermal vent (Rathgeber et al. 2004). The spirilla shapes we observed have not yet been reported in isolates.

The vertical pattern of AAPs relative to Chl *a* (Fig. 4) is similar to that seen by Kolber et al. (2001) in the more productive northeast Pacific waters; however, they observed a subsurface maximum in total bacteria that we did not see. Yurkov and Beatty (1998) found that the growth of AAP bacteria in culture is inhibited by as little as 20 μmol quanta m^{-2} s^{-1} of light irradiance. This light level is generally exceeded on sunny days in the top 100 m of the Sargasso Sea (attenuation, $K_d = 0.03$ m^{-1}, surface irradiance 10^3 μmol quanta m^{-2} s^{-1}) or in the top 10 m in shelf waters ($K_d = 0.4$ m^{-1}) (Kirk 1994). Such inhibition may be occurring but is not likely in the populations of AAPs observed, since they show near-surface maxima in their depth profiles. This may be indicative of differences between the cultured and wild types of AAPs. Ocean microbes vertically partition the environment in distinct ways based on their nutrient metabolism and photophysiology (Glover et al. 1986; Kana and Glibert 1987; Rocap et al. 2003). Bacteria with AAP photophysiology are clearly a part of this microbial phototrophic community. Their physiologies may influence the environment as well through competition for nutrients and reductants, production of bioactive compounds, and selective spectral absorption of light. These potential interactions require further investigation.

Temperate coastal systems have strong seasonal variations attributable to temperature and stratification cycles. For example, in March, waters in the Gulf of Maine can be well mixed or partially stratified (Townsend et al. 1992) and are near the lowest annual temperatures. Our results show a large difference in the AAP abundances between October and March in the Gulf of Maine samples. The mixed layer was deeper in March, but dilution by mixing alone could not account for the observed difference. The factors that cause the difference are probably the same factors that drive seasonal phytoplankton succession. The chlorophyll levels in March were not low, so the spring bloom, dominated by diatoms, had probably begun. Picophytoplankton abundances increase in later spring and peak in summer, approximately following the temperature curve. They appear to prefer stratified conditions and growth on recycled nutrients. AAP abundance could follow a similar seasonal pattern.

For the March cruise, during which we measured BChl *a* pigment concentrations, we observed a strong correlation between BChl *a* and Chl *a*. The ratio of BChl *a* to Chl *a* for

this sample set did not decline with increasing Chl *a*, as was observed in Pacific surface waters (Goericke 2002). Our observed BChl *a* pigment concentrations, ranging from undetectable in deep water to 2.4 ng L^{-1}, are on the low end of the range found in the southern California current system of the northeast Pacific Ocean (Goericke 2002), where values ranged from 0.26 to 4.8 ng L^{-1}. Kolber et al. (2001) reported offshore north Pacific concentrations ranging from about 0.30 to 5.8 ng L^{-1}. When converted to pigment per cell, our values were higher than those reported by Kolber et al. (2001)—their data yielded a cell quota of 0.0098 fg cell $^{-1}$, just half of our lowest value (Table 4). The high variation we observed in cell pigment content could be due to both the diversity of AAP bacterial types and photophysiological adaptation. The pigment content calculation is also subject to the combined errors of the pigment and cell count methods, so it is useful to compare the BChl *a* content values of AAPs with the pigment content of *Prochlorococcus*, another prokaryotic phototroph that occurs with AAPs in oceanic samples and has a very low cellular content of photopigment in surface waters. Divinyl Chl $a+b$ ranged from 0.06 to 0.22 fg cell^{-1} in *Prochlorococcus* in surface (<40 m) tropical Atlantic waters (data from fig. 6 of Veldhuis and Kraay [2004]). Pigment content of *Prochlorococcus* increased greatly with depth, however, with many samples below 100 m having greater than 10 fg cell^{-1} and a maximum value of 22 fg cell^{-1}—a 350× range. Assuming a *Prochlorococcus* cell volume of 0.27 μm^3, the surface (<40-m) range of pigment normalized to cell biovolume is about 0.2–0.8 fg μm^{-3}. Our values for BChl *a* normalized to cell volume (fg μm^{-3}) were comparable to these, ranging from 0.16 to 1.3 fg BChl *a* μm^{-3}. We observed a correlation (r^2) between AAP cell counts and BChl *a* concentrations of 0.36, meaning that they share about 36% of the observed variation. Differences in pigment concentration per cell probably account for most of the remaining variation (excluding sampling and measurement error).

Our observed correlation between AAPs and Chl *a* in the warmer month indicates that the distribution of these cells is controlled by temperature and inorganic and organic nutrients, rather than specific adaptation to oligotrophic habitats. AAP bacteria may act as a sunlight-accelerated shunt of energy between the large pool of oceanic dissolved organic matter and higher trophic levels. Average AAP cells were between 1.3 and 2.6 times larger in biovolume than the average of the total bacteria, and the AAPs from the Sargasso Sea were morphologically diverse. Larger bacteria are preferentially grazed by heterotrophic protists in the ocean (Anderson et al. 1986; Gonzalez et al. 1990; Monger and Landry 1992), so AAPs are likely to experience high grazing mortality and, consequently, high turnover rates compared to the other, smaller bacteria. If this is true, their role in the ocean carbon cycle could be greater than their abundances imply.

References

ANDERSON, A., U. LARSSON, AND A. HAGSTROM. 1986. Size-selective grazing by a microflagellate on pelagic bacteria. Mar. Ecol. Prog. Ser. **33:** 51–57.

BÉJÁ, O., AND OTHERS. 2002. Unsuspected diversity among marine aerobic anoxygenic phototrophs. Nature **415:** 630–633.

BRITSCHGI, T. B., AND S. J. GIOVANONNI. 1991. Phylogenetic analysis of a natural marine bacterioplankton population by rRNA gene cloning and sequencing. Appl. Environ. Microbiol. **57:** 1707–1713.

DUCKLOW, H. W., D. C. SMITH, L. CAMPBELL, M. R. LANDRY, H. L. QUINBY, G. F. STEWARD, AND F. AZAM. 2001. Heterotrophic bacterioplankton in the Arabian Sea: Basinwide response to year-round high primary productivity. Deep-Sea Res. II **48:** 1303–1323.

FENCHEL, T., G. M. KING, AND T. H. BLACKBURN. 1998. Bacterial biogeochemistry: The ecophysiology of mineral cycling, 2nd ed. Academic Press.

FRY, J. C. 1988. Determination of biomass, p. 27–72. *In* B. Austin [ed.], Methods in aquatic bacteriology. Wiley.

GLOVER, H. E., M. D. KELLER, AND R. L. GUILLARD. 1986. Light quality and oceanic ultraphytoplankters. Nature **319:** 142–143.

GOERICKE, R. 2002. Bacteriochlorophyll *a* in the ocean: Is anoxygenic bacterial photosynthesis important? Limnol. Oceanogr. **47:** 290–295.

GONZALEZ, J. M., E. B. SHERR, AND B. F. SHERR. 1990. Size-selective grazing on bacteria by natural assemblages of estuarine flagellates and ciliates. Appl. Environ. Microbiol. **56:** 583–589.

GUNDERSEN, K., M. HELDAL, S. NORLAND, D. A. PURDIE, AND A. H. KNAP. 2002. Elemental C, N, and P cell content of individual bacteria collected at the Bermuda Atlantic Time-Series Study (BATS) site. Limnol. Oceanogr. **47:** 1525–1530.

KANA, T. M., AND P. M. GLIBERT. 1987. Effect of irradiances up to 2000 μE m^{-2} s^{-1} on marine *Synechococcus* WH7803-II. Photosynthetic responses and mechanisms. Deep-Sea Res. **34:** 497–516.

KARL, D. M. 2002. Hidden in a sea of microbes. Nature **415:** 590–591.

KARNER, M. B., E. F. DELONG, AND D. M. KARL. 2001. Archaeal dominance in the mesopelagic zone of the Pacific Ocean. Nature **409:** 507–510.

KIRK, J. T. O. 1994. Light and photosynthesis in aquatic ecosystems, 2nd ed. Cambridge Univ. Press.

KOBLIZEK, M., AND OTHERS. 2003. Isolation and characterization of *Erythrobacter* sp. strains from the upper ocean. Arch. Microbiol. **180:** 327–338.

KOLBER, Z. S., C. L. VAN DOVER, R. A. NIEDERMAN, AND P. G. FALKOWSKI. 2000. Bacterial photosynthesis in surface waters of the open ocean. Nature **407:** 177–179.

———, AND OTHERS. 2001. Contribution of aerobic photoheterotrophic bacteria to the carbon cycle in the ocean. Science **292:** 2492–2495.

MONGER, B. C., AND M. R. LANDRY. 1992. Size-selective grazing by heterotrophic nanoflagellates: An analysis using live-stained bacteria and dual-beam flow cytometry. Arch. Hydrobiol. **37:** 173–185.

PARSONS, T. R., Y. MAITA, AND C. M. LALLI. 1984. A manual of chemical and biological methods for seawater analysis. Pergamon.

PORTER, K. G., AND Y. S. FEIG. 1980. The use of DAPI for identifying and counting aquatic microflora. Limnol. Oceanogr. **25:** 943–948.

POSCH, T., M. LOFERER-KRÖBACHER, G. GAO, A. ALFREIDER, J. PERNTHALER, AND R. PSENNER. 2001. Precision of bacterioplankton biomass determination: A comparison of two fluorescent dyes, and of allometric and linear volume-to-carbon conversion factors. Aquat. Microb. Ecol. **25:** 55–63.

RATHGEBER, C., J. T. BEATTY, AND V. YURKOV. 2004. Aerobic phototrophic bacteria: New evidence for the diversity, ecological

importance and applied potential of this previously overlooked group. Photosynthesis Res. **81:** 113–128.

ROCAP, G., AND OTHERS. 2003. Genomic divergence in two *Prochlorococcus* ecotypes reflects oceanic niche differentiation. Nature **424:** 1042–1047.

SCHWALBACH, M. S., AND J. A. FUHRMAN. 2005. Wide-ranging abundances of aerobic anoxygenic phototrophic bacteria in the world ocean revealed by epifluorescence microscopy and quantitative PCR. Limnol. Oceanogr. **50:** 620–628.

SHIBA, T., U. SIMIDU, AND N. TAGA. 1979. Distribution of aerobic bacteria which contain bacteriochlorophyll *a.* Appl. Environ. Microbiol. **38:** 43–45.

SIERACKI, M. E., T. L. CUCCI, AND J. NICINSKI. 1999. Flow cytometric analysis of 5-cyano-2,3-ditoyl tetrazolium chloride activity of marine bacterioplankton in dilution cultures. Appl. Environ. Microbiol. **65:** 2409–2417.

———, E. HAUGEN, AND T. L. CUCCI. 1995. Overestimation of heterotrophic bacteria in the Sargasso Sea: Direct evidence by flow and imaging cytometry. Deep-Sea Res. **42:** 1399–1409.

———, C. L. VILES, AND K. L. WEBB. 1989. Algorithm to estimate cell biovolume using image analyzed microscopy. Cytometry **10:** 551–557.

STEINBERG, D. K., C. A. CARLSON, N. R. BATES, R. J. JOHNSON, A. F. MICHAELS, AND A. H. KNAP. 2001. Overview of the US JGOFS Bermuda Atlantic Time-Series Study (BATS): A decade-scale look at ocean biology and biogeochemistry. Deep-Sea Res. II **48:** 1405–1447.

TOWNSEND, D. W., M. D. KELLER, M. E. SIERACKI, AND S. G. ACKLESON. 1992. Spring phytoplankton blooms in the absence of vertical water column stratification. Nature **360:** 59–62.

VELDHUIS, M. J. W., AND G. W. KRAAY. 2004. Phytoplankton in the subtropical Atlantic Ocean: Towards a better assessment of biomass and composition. Deep-Sea Res. I **51:** 507–530.

VILES, C. L., AND M. E. SIERACKI. 1992. Measurement of marine picoplankton cell size by using a cooled, charge-coupled device camera with image-analyzed fluorescence microscopy. Appl. Environ. Microbiol. **58:** 584–592.

YURKOV, V. V., AND J. T. BEATTY. 1998. Aerobic anoxygenic phototrophic bacteria. Microbiol. Mol. Biol. Rev. **62:** 695–724.

Received: 2 December 2004
Accepted: 19 July 2005
Amended: 6 September 2005